Volume 1 | Number 1 | Jan 2013 | Pages 1–100

Nanoscale

www.rsc.org/nanoscale

Interaction of PLGA nanoparticles with blood components: protein adsorption,

coagulation, activation of the complement system and hemolysis studies

Cristina Fornaguera[a*], Gabriela Calderó[a], Montserrat Mitjans[b], Maria Pilar Vinardell[b],

Conxita Solans[a], Christine Vauthier[c]

[a]Institute of Advanced Chemistry of Catalonia IQAC/CSIC and CIBER of Bioengineering, Biomaterials and Nanomedicine (CIBER-BBN), C/Jordi Girona, 18-26, Barcelona, 08034, Spain.

[b]Physiology department, Pharmacy Faculty, Universitat de Barcelona, Av. Joan XXIII, s/n, Barcelona, 08028, Spain.

[c]Université Paris-Sud, Faculté de Pharmacie, CNRS UMR 8612, Institute Galien Paris-Sud, 5 rue J.B. Clément, 92296, France.

*Corresponding author :

Adress: C/ Jordi Girona, 18-26, 08034, Barcelona, Spain
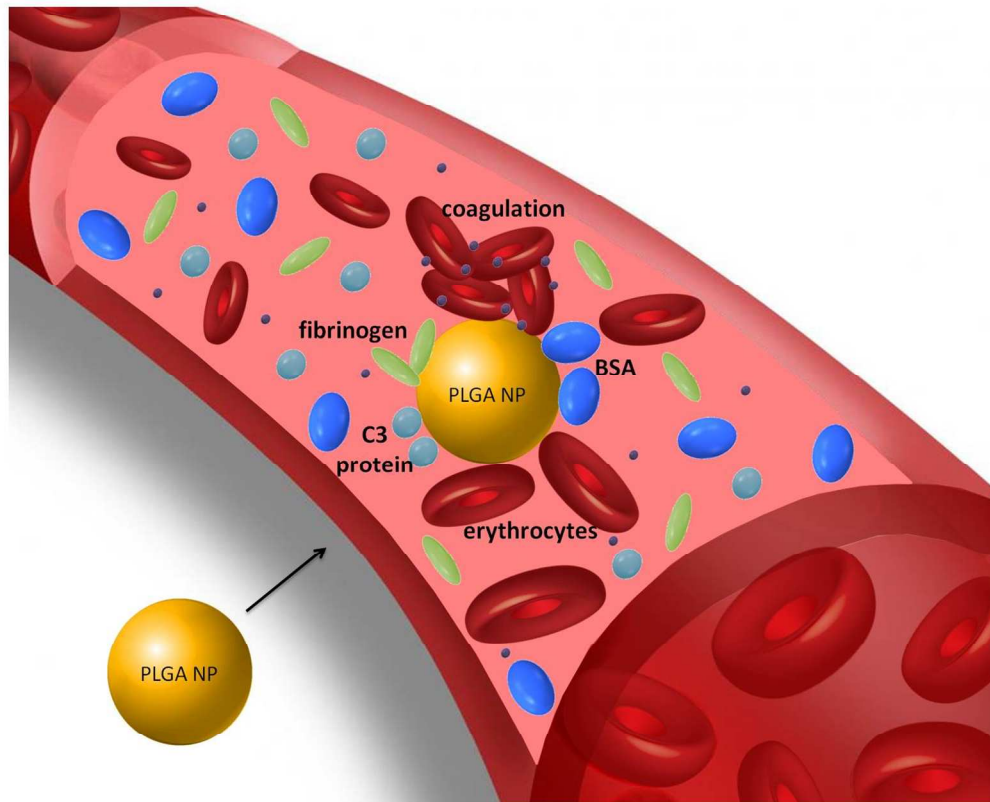
Telephone: +34-934006100 ext.2302

Fax : +342045904

E-mail adress: cristina.fornaguera@iqac.csic.es (permanent : cfornaguera@gmail.com)

Table of contents

Schematic representation of PLGA nanoparticles interaction with blood components when

they enter the bloodstream.

1

Abstract

The intravenous administration of poly(lactic-co-glycolic) acid (PLGA) nanoparticles has been widely reported as a promising alternative to delivery drugs to specific cells. However, studies on their interaction with diverse blood components combining different techniques are still missing. Therefore, in the present work, the interaction of PLGA nanoparticles with blood components was described using different complementary techniques. The influence of different encapsulated compounds / functionalization agents on these interactions was also reported. It is worth noting that all these techniques can be

simply performed, without the need of highly sophisticated apparatus or skills. Moreover, their transference to industries and application of quality control could be easily performed. Serum albumin was adsorbed onto all types of tested nanoparticles. The saturation concentration was dependent on the nanoparticle size. In contrast, fibrinogen aggregation was dependent on nanoparticle surfaces charge. The complement activation was also influenced by the nanoparticle functionalization; the presence of a functionalization agent increased complement activation, while the addition of an encapsulated compound only produced a slight increase. None of the nanoparticles influenced the coagulation cascade at low concentrations. However, at high concentration, cationized nanoparticles did activate the coagulation cascade. Interaction of nanoparticles with erythrocytes did not reveal any hemolysis. Interactions of PLGA nanoparticles with blood proteins depended both on the nanoparticle properties and the protein studied. Independently of their loading /surface functionalization, PLGA nanoparticles did not influence the coagulation cascade and did not induce hemolysis of erythrocytes; they could be defined as safe concerning induction of embolization and cell lysis.

1. **Introduction**

Polymeric nanoparticles have been widely studied and confirmed as nanomedicines for diagnostic and therapeutic purposes [1-5]. The intravenous route of administration allows systemic delivery of drugs [6], to achieve a specific and targeted drug delivery with nanoparticles to many target organs with specifically designed nanoparticles [7-9]. Previous studies have pointed out the importance of studying of, at least, three factors when nanoparticles are intended to be administered for intravenous injection: a) the protein adsorption pattern; b) the influence on the coagulation cascade; and c) their hemolytic character, as recommended by the ISO-10993 [2,10]. However, the literature is dispersed and only few studies reported the three factors for a series of identical nanoparticles [2,10-11].

Intravenously injected nanoparticles arrive into a solution of proteins at high concentration (62 − 84 g/L) [2,12]. Therefore, the protein adsorption onto nanoparticle surface is one of the first events that takes place when nanoparticles enter the blood stream. This phenomenon, termed "opsonization", will contribute to determine the nanoparticle fate in the body, which depends on the protein pattern (type and amount of proteins) adsorbed onto each type of nanoparticles [2,8,12-14]. The adsorbed protein pattern depends, in turn, on nanoparticle physico-chemical properties, such as their size, charge and surface composition [2,8,10,13,15]. The most abundant protein in the blood is the serum albumin, which is present at a concentration of 40g/L. Consequently, serum albumin will be one of the main proteins that adsorb first onto the nanoparticle surface. Following, other proteins, such as fibrinogen, will displace or bound the adsorbed

albumin. The body recognition of the protein adsorption will be the cause of the immune system activation, thus producing an activation of the complement cascade, among others [2,12,14]. While activation of the complement cascade can be triggered by different signals involving different proteins, the protein C3 always acts when this cascade is activated. Its activation represents a key event of the complement cascade, which will produce the elimination of the nanoparticles that triggered the activation [12]. It seems that some correlation exists between low protein binding capacity of nanoparticles and their low potential to activate the complement system [2,16]. Having nanoparticles with this property is desired, because they remain in the blood circulation, thus enabling their distribution towards target tissues. It is also highly desired in regard with the safety, as a serious adverse reaction called CAPRA could appear. CAPRA produces a variety of symptoms similar to those of a hypersensitivity reaction, which are due to the recognition of nanomedicines by the immune system leading to an activation of the complement system [17-18]. Although this effect is difficult to study *in vivo*, activation of the complement system induced by nanoparticles can be studied by *in vitro* tests.

The protein adsorption pattern onto nanoparticle surface could also influence biological responses such as coagulation [19]. The coagulation cascade (or blood clotting) is a highly complex process, activated by the fibrinogen and involving many other proteins [10,20-21]. It is divided into two pathways: the intrinsic or contact activation pathway, activated by antigen-antibody complexes due to damage on a blood vessel surface, and the extrinsic or tissue pathway, antibody independent; finishing both in a common pathway. Previous studies demonstrated that intravenously injected polymeric nanoparticles could modify

the coagulation time by both pathways. Obviously, safe nanoparticles are expected to have no effect on the coagulation time. Shorter coagulation times could induce toxicity by formation of thrombus that could partially or completely occlude blood vessels, while an anticoagulant effect (longer coagulation times) would cause hemorrhage [2]. The last important parameter to study is hemolysis. The term hemolysis is referred to the disruption of the red blood cells (erythrocytes). The cause of erythrocytes hemolysis is another indication of nanoparticle toxicity in the blood, which concerns the integrity of the red blood cells [2,22]. Therefore, the results of the hemolytic nanoparticle activity will be an indication of their interaction with cell membrane and toxicity behavior towards cells [10].

In the present work, we chose poly(lactic-co-glycolic) acid (PLGA) nanoparticles because they are extensively studied as colloidal drug carriers for intravenous administration of drugs, since PLGA is a FDA approved polymer. Series of PLGA nanoparticles were studied, with different encapsulated compounds (loperamide hydrochloride as a model drug and Coumarin 6 as a model fluorescent molecule) and / or surface functionalizations (cationic carbosilane dendron and a model antibody). Although there are many studies reporting the interaction of blood proteins with PLGA nanoparticles [23-28], none of the work published so far have considered in a single report PLGA interaction with diverse blood components as a function of the loading / functionalization. Thus, in the present work, we aimed to contribute to improve the knowledge of PLGA nanoparticles interaction with blood complements: serum albumin and fibrinogen as model proteins, the activation of the complement protein C3 as indication of the activation of the complement system, the

interaction with the coagulation cascade and the hemolytic character of nanoparticles. In addition, we attempted to find out if an encapsulated compound or a modification of the nanoparticle surface will produce changes on their interaction with blood components.

It is noteworthy that these nanoparticles were prepared by the nano-emulsification approach, using the phase inversion composition method (PIC) [29] to prepare nano-emulsions. This method is advantageous for obtaining nanoparticles with very small nanometric sizes [30-31]. Smaller sizes are advantageous in terms of enhanced stability of the nanoparticle dispersions, as well as in avoiding blood vessels embolization and detection by the immune system followed by nanoparticle clearance [9,25,32-36].

2. Results

2.1. Preparation and characterization of nanoparticles

Nanoparticles were characterized by means of size and surface charge determination in different dispersion buffers, to assess their behavior in the different buffers used for the experimentation reported in the present work. The phosphate buffered saline (PBS) was used as the dispersion buffer to keep nanoparticles and to perform most of the experiments (fibrinogen and BSA adsorption, coagulation and hemolysis). The veronal buffered saline (VBS^{2+}), together with human serum (HS) was used for the complement activation studies. Nevertheless, the stability of nanoparticles in VBS^{2+}, without HS, was also studied with the aim to differentiate the effect produced by this buffer to that of the HS.

Nanoparticles physico-chemical characteristics are presented in Table 2. Non-loaded non-functionalized nanoparticles (NP) showed hydrodynamic radii of around 20 nm, which was only slightly increased when Coumarin 6 (C6) was incorporated and when nanoparticles were functionalized either with G2SN dendron or with 8D3 antibody. However, loperamide loading inside of nanoparticles produced a considerable increase in the nanoparticle size up to 100nm in PBS buffer. This nanoparticle size increase with loperamide encapsulation was attributed to the oil component of the template nano-emulsion which was different from the rest of the systems due to solubility requirements (unpublished results).

NP showed negative surface charges, of around -20mV. The incorporation of an encapsulated compound resulted in less negative surface charges, when the compound was Coumarin 6, while it was more negative when it was loperamide, using PBS buffer. NP(8D3) showed negative charges also, but they were less negative. As expected and previously reported [31], the covalent binding of the G2SN dendron resulted in nanoparticles with a cationic surface since G2SN dendrons are cationic molecules, independently of the nanoparticles loading.

Table 2 also shows the stability of nanoparticles in the above-mentioned buffers, after 1 hour of incubation, the maximum experimental required time for complement activation study, by means of hydrodynamic sizes and ζ potential measurements, compared with initial values. The hydrodynamic radii of all studied nanoparticles (Table 2a) remain constant when nanoparticles are dispersed in both buffers (PBS and VBS^{2+}), after 1 hour of

8

incubation, at 37ºC. Comparing both buffers, the nanoparticle sizes did not varied markedly, with the exception of loperamide-loaded nanoparticles, where a nanoparticle size decrease of around 40nm was found in VBS^{2+}, as compared with PBS buffer. However, the addition of HS to the VBS^{2+} dispersion media produced a remarkable nanoparticle size increase in most of the types studied, just after its addition (t=0). Moreover, aggregates were clearly formed in most nanoparticle types (NP(G2SN), NP(C6), NP(C6,G2SN) and NP(8D3)); thus, it was not possible to characterize them after 1 hour of incubation. Those non-aggregating nanoparticles (NP, NP(LOP) and NP(LOP,G2SN)) showed lower sizes after 1 hour of incubation with VBS^{2+} and HS, as compared with their initial sizes when dispersed in the same buffer.

Concerning the ζ potential stability, when nanoparticles were dispersed in PBS and VBS^{2+} buffers (Table 2b), it did not varied after 1h incubation. However, the addition of HS produced a shift of the ζ potential of all types of nanoparticles to lower negative charges. Those nanoparticles with negative ζ potential in PBS and VBS^{2+} buffers had surface charges of around -10mV, while those with positive charges shifted to negative charges around -2mV. Therefore, the presence of HS in the dispersion media affected both, the nanoparticle sizes and their surface charges.

Table 2: Characterization of: a) nanoparticles size (hydrodynamic radii, in nm); and b) surface charge (ζ potential, in mV) of diverse types of the as-prepared nanoparticles dispersed in different buffers.

a)

Identification	Hydrodynamic droplet radii (nm)					
	PBS		VBS^{2+}		VBS^{2+} + HS	
	t = 0	t = 1h	t = 0	t = 1h	t = 0	t = 1h
NP	20 ± 3	17 ± 4	17 ± 0	17 ± 0	66 ± 2	60 ± 1
NP(G2SN)	26 ± 9	25 ± 2	66 ± 3	64 ± 2	Agregated	Agregated
NP(C6)	23 ± 1	24 ± 2	20 ± 0	26 ± 1	Agregated	Agregated
NP(C6,G2SN)	24 ± 1	27 ± 1	27 ± 7	25 ± 5	Agregated	Agregated
NP(LOP)	100 ± 5	101 ± 6	44 ± 2	45 ± 1	281 ± 12	157 ± 24
NP(LOP,G2SN)	98 ± 1	98 ± 2	69 ± 5	66 ± 3	760 ± 43	530 ± 99
NP(8D3)	21 ± 2	23 ± 3	23 ± 3	24 ± 11	Agregated	Agregated

b)

Identification	ζ potential (mV)					
	PBS		VBS^{2+}		VBS^{2+} + HS	
	t = 0	t = 1h	t = 0	t = 1h	t = 0	t = 1h
NP	-22 ± 1	-20 ± 2	-14 ± 1	-23 ± 1	-13 ± 1	-13 ± 0
NP(G2SN)	33 ± 2	32 ± 1	26 ± 1	22 ± 1	Agregated	Agregated
NP(C6)	-15 ± 3	-13 ± 4	-28 ± 2	-30 ± 1	Agregated	Agregated
NP(C6,G2SN)	21 ± 2	24 ± 3	22 ± 1	26 ± 1	Agregated	Agregated
NP(LOP)	-27 ± 2	-25 ± 3	-21 ± 0	-23 ± 3	-13 ± 1	-12 ± 1
NP(LOP,G2SN)	28 ± 3	34 ± 2	32 ± 2	31 ± 1	-1 ± 0	-2 ± 0
NP(8D3)	-15 ± 3	-15 ± 1	-26 ± 1	-23 ± 2	-16 ± 1	-15 ± 1

10
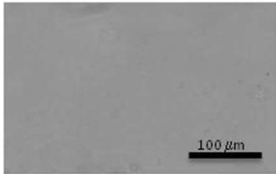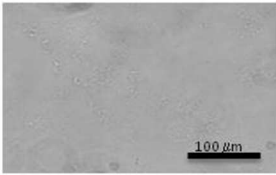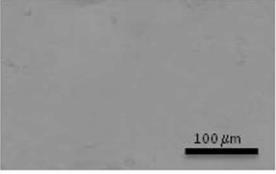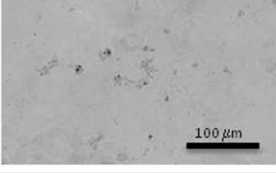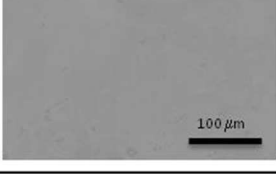
2.2. Interaction of nanoparticles with model proteins

2.2.1. **Interaction with fibrinogen**

The nanoparticle aggregation in the presence of fibrinogen was studied by visual macroscopic observations of nanoparticle dispersions. Results are presented in Table 3. When fibrinogen was added to the nanoparticle dispersions, those containing the dendron functionalization rapidly sedimented, while others remained apparently stable ov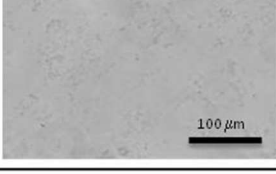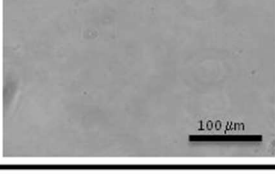er a period of time of 1h. Their macroscopic stability was verified by optical microcopy. Size and ζ potential measurements were performed with those that appeared homogeneous by optic microscopy.

Results are also presented in Table 3, where initial sizes in PBS are also included for comparative purposes. Hydrodynamic radii were slightly increased for all nanoparticles except for those containing loperamide, where a size reduction was observed. Surface charges of non-aggregating nanoparticles remained negative after fibrinogen incubation (Table 3), as expected, since the net charge of fibrinogen at the studied pH (7.4) is negative. However, in several nanoparticle dispersions, the ζ potential varied after fibrinogen incubation, which could be an indication of fibrinogen interaction with those nanoparticles, although they did not aggregate.

Table 3: Nanoparticle dispersion characterization (Visual aspect, micrographs, hydrodynamic radii (nm) and ζ potential (mV)) of nanoparticle dispersions after their incubation with 2mg/mL of fibrinogen, in PBS buffer, for 1 hour.

Sample	Visual aspect	Micrography	Hydrodynamic radii (nm)	ζ potential (mV)
NP		100 μm	30 ± 5	-10 ± 1
NP(G2SN)		100 μm	Aggregated	Aggregated
NP(C6)		100 μm	29 ± 2	-13 ± 1
NP(C6,G2SN)		100 μm	Aggregated	Aggregated
NP(LOP)		100 μm	77 ± 5	-18 ± 2
NP(LOP,G2SN)		100 μm	Aggregated	Aggregated
NP(8D3)		100 μm	32 ± 4	-15 ± 2

2.2.2. **Interaction with BSA**

The adsorption of bovine serum albumin (BSA) was also studied for all nanoparticles. For this evaluation, it was postulated that the ζ potential of the nanoparticles would change in case of adsorption of BSA. No change in ζ potential was observed after addition of increasing BSA concentrations in NP and NP(C6). ζ potential of nanoparticles incubated with BSA varied by increasing the BSA concentration up to a plateau value (Figure 1). The ζ potential of nanoparticles without BSA was positive for those nanoparticles containing G2SN functionalization, as expected; while it was negative for the other dispersions. At low BSA concentrations, the adsorbed BSA (corresponding to the y axis) was similar to the initial BSA concentration (x axis), indicating a high adsorption for low BSA concentrations. For those nanoparticles, the ζ potential obtained at the plateau varied from -18 to -10 mV independently on the original ζ potential. The BSA saturation took place at BSA concentrations lower than 10 mg/mL in all cases, except for NP(LOP). Therefore, the BSA concentrations of saturation found by this technique were typically below 10mg/mL. However, the BSA saturation concentration was different between different nanoparticles dispersions, thus indicating a dependence of the BSA concentration of saturation on the nanoparticle loading / functionalization.
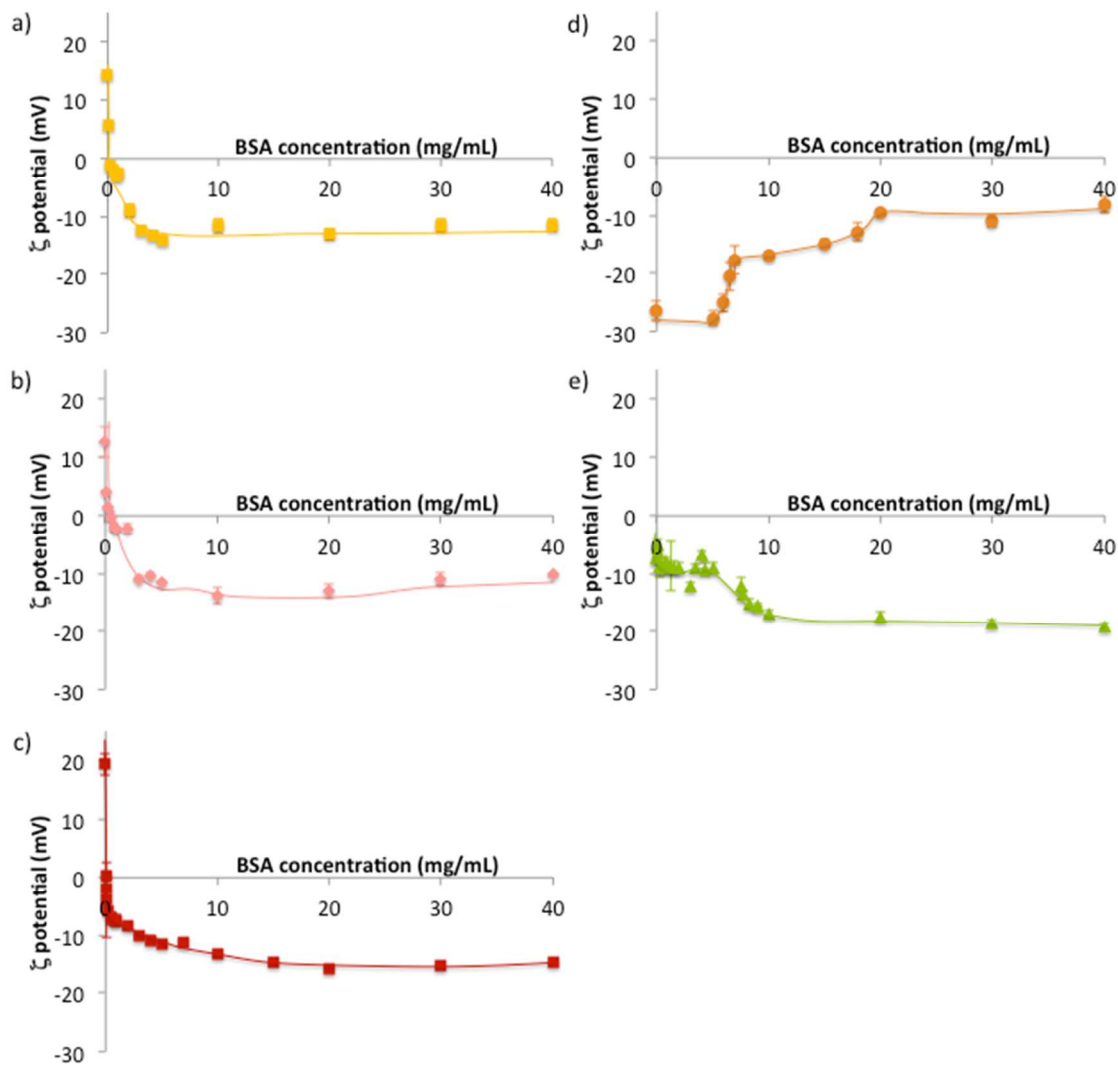
Figure 1: BSA adsorption isotherms by means of the ζ potential measurement at increasing concentrations of BSA (mg/mL), in PBS buffer. a) NP(G2SN); b) NP(C6,G2SN); c) NP(LOP,G2SN); d)NP(LOP) and e)NP(8D3).

2.3. **Interaction of nanoparticles with the coagulation cascade**

The influence of nanoparticles on the coagulation cascade is another important factor that must be studied when nanoparticles are intended for the intravenous administration [2].

14

In the present work, blood from healthy donors was used for this study; specifically the isolated plasma fraction was used. Results were tested by means of the activated partial thromboplastin time (APTT) and the prothrombin time (PT), as a function of the nanoparticle type and concentration. As Figure 2a shows, the APTT values for all nanoparticle dispersions are in the physiological range at lower nanoparticle concentrations. However, at increasing the nanoparticle concentration, an increase in the APTT values was found. This increase was slight for most nanoparticles, as compared with that of NP(G2SN). Similar results were found for the PT times (Figure 2b), although time increase was noticeable only for NP(G2SN) nanoparticles. The normal APTT values range between 25 – 35 seconds, while the basal values for the PT time range between 12 – 15 seconds [19,21]. Therefore, at the highest concentration tested (3mg/mL), NP(G2SN) produced an anticoagulant effect, as reported by both coagulation parameters studied (Figure 2). For NP and NP(C6) a slight increase in the APTT values was also found but they cannot be defined as anticoagulants, since the PT times were within the normality (Figure 2). All nanoparticles studied did not influence the coagulation times at concentrations up to 1mg/mL, the usual concentration used to perform coagulation studies [2].
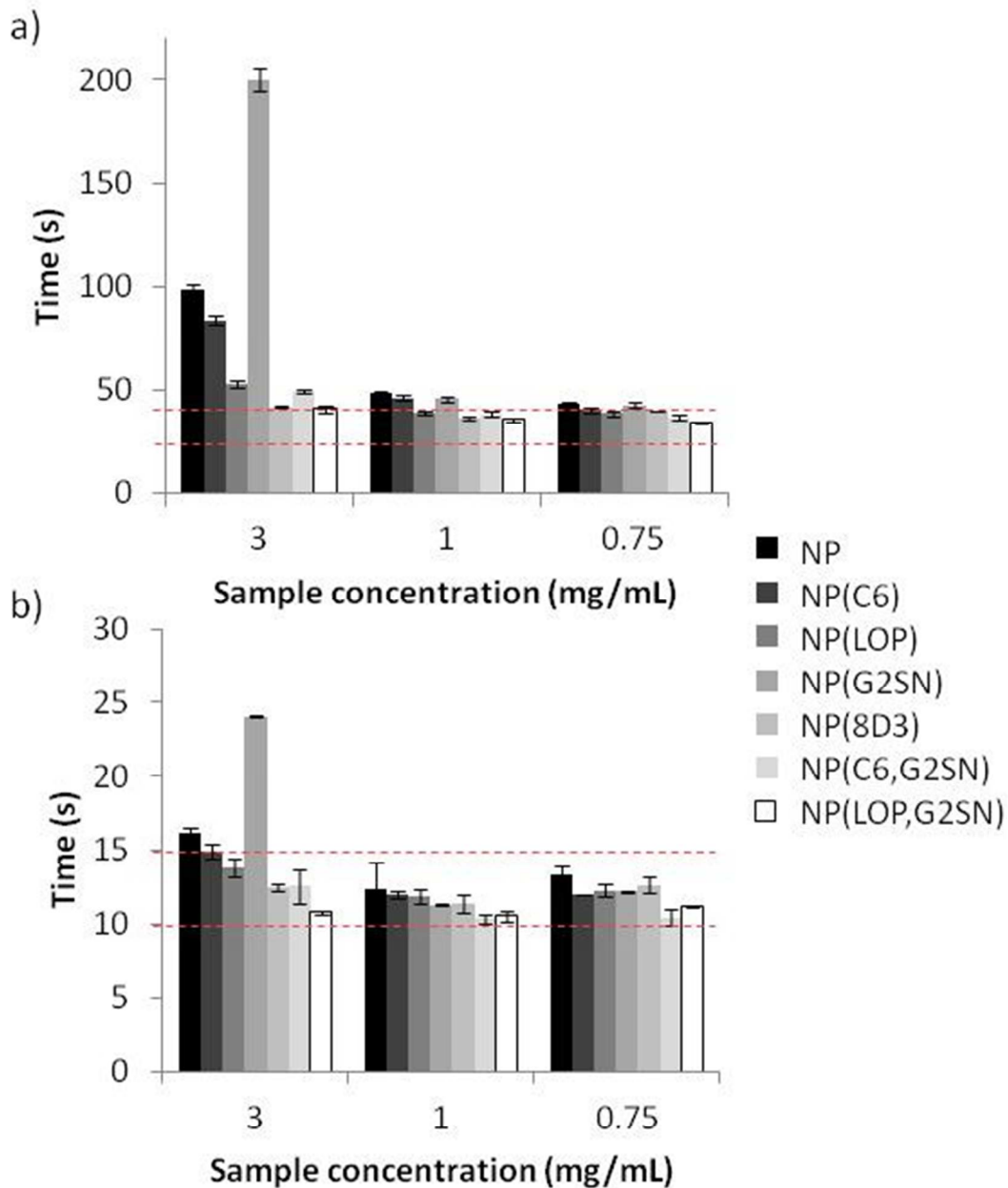
Figure 2: Coagulation time as a function of the simple type and concentration. Figure a)

represents the APTT results while b) corresponds to the PT results. Grey zones correspond

to the expected times for healthy donors. Mean values ± SD of at least three independent

experiments from different donors.

2.4. **Interaction of nanoparticles with the complement cascade**

The activation of the complement cascade was studied by measuring the activation of the C3 complement protein, using 2D immunoelectrophoresis. The results, presented in Table 4, given as normalized percentages of C3 activation, show that NP were really weak activators of the complement system (activation of around 5%). The addition of an encapsulated compound produced an increase on the C3 activation, up to values around 20 – 25%. Furthermore, nanoparticle functionalization also produced an increase on the complement activation. NP(G2SN) showed percentages of activation around 40%, while these percentages were increased up to 60% for NP(8D3). It is worth remarkable that the shape of the electrophoresis profiles (Figure S1, SI) depended on the functionalization agent.
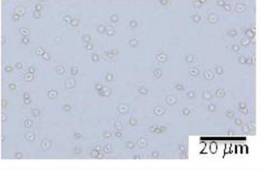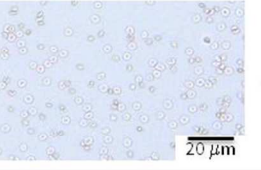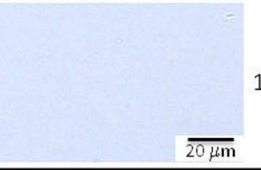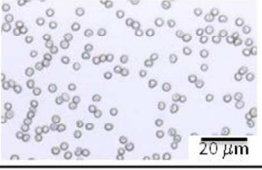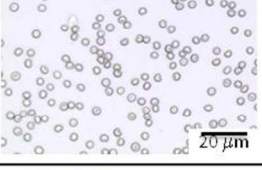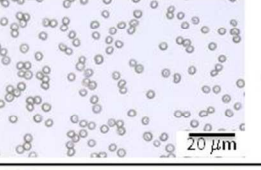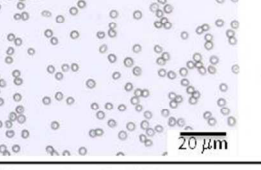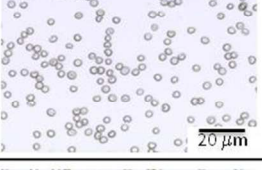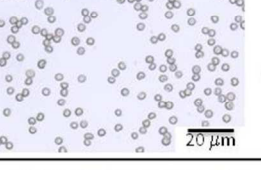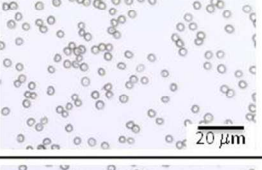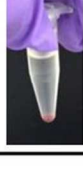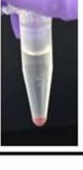
Table 4: Percentage of C3 complement protein activation for nanoparticles with different functionalizations and loadings. Mean values ± SD of at least three independent experiments.

17

Nanoparticle type	Percentage of C3 activation
NP	5 ± 1
NP(G2SN)	39 ± 2
NP(C6)	25 ± 1
NP(C6,G2SN)	35 ± 1
NP(LOP)	19 ± 2
NP(LOP,G2SN)	16 ± 1
NP(8D3)	61 ± 1

2.5. **Determination of the hemolysis**

These experiments were performed to evaluate the toxicity of nanoparticles with blood cells. The results are shown in Table 5. All nanoparticle dispersions, studied at the as-prepared concentration (3mg/mL), were non-hemolytic after 10 minutes and 24 hours of incubation with erythrocytes, since hemolysis percentages were nearly null for all nanoparticles. The results allowed stating the non-cytotoxic character of the formulated nanoparticles, independently of their loading or functionalization. Furthermore, the integrity of erythrocytes was confirmed by microscopic observation (Table 5).

Table 5: Nanoparticle hemolysis (%) of the nanoparticle dispersions (3mg/mL), after 10 min and 24 h of incubation. Mean values ± SD of at least three independent experiments from different donors.

Sample	Incubation time = 10 min			Incubation time = 24h		
	Visual aspect	Micrography	Hemolysis (%)	Visual aspect	Micrography	Hemolysis (%)
Control – (PBS)			0.00 ± 0.00			0.00 ± 0.00
Control + (Water)			100.00 ± 0.54			100.00 ± 0.17
NP			0.00 ± 0.00			0.00 ± 0.00
NP(G2SN)			0.00 ± 0.00			0.00 ± 0.00
NP(C6)			0.00 ± 0.00			0.00 ± 0.00
NP(C6,G2SN)			0.00 ± 0.00			0.00 ± 0.00
NP(LOP)			2.43 ± 0.08			0.00 ± 0.00
NP(LOP,G2SN)			3,01 ± 0.02			0.00 ± 0.00
NP(8D3)			0.00 ± 0.00			0.00 ± 0.00

3. **Discussion**

The protein adsorption onto nanoparticle surface is a well-known and widely studied phenomenon that takes place when nanoparticles enter in the bloodstream [2,15-16]. In the present work, PLGA nanoparticles with different loadings and functionalizations were studied and compared with the aim to better understand the effect on adsorbed proteins, of an encapsulated drug (loperamide) or fluorescent dye (Coumarin 6), of a functionalizing element covalently attached to nanoparticle surface (dendron G2SN or 8D3 antibody) or a combination between them. All these nanoparticles showed sizes (Table 2) in the range of intravenously administrable nanosystems (below 1 µm) in the as-prepared buffer (PBS) [6,25]. Therefore, the study of their interaction with blood components was considered of interest.

An initial key point is the nanoparticle blood compatibility. The non-hemolytic character of all types of nanoparticles confirms their hemocompatibility with erythrocytes. Comparing with previous studies reporting PLGA nanoparticles, *Kim et al.,* [27] found really higher hemolytic percentages (around 80%) than ours, which were attributed to the presence of a non-ionic surfactant (lauric acid sodium salt), at nanoparticle concentrations equivalent to ours (between 1 to 10mg/g vs our 3mg/g). They achieved a marked reduction of the hemolysis after the nanoparticles were coated with poly(ethyleneglycol), reaching to values around 20%. Nevertheless, most studies on PLGA nanoparticles did not produced hemolysis [11,39], as for our results. In our study, although nanoparticles were formulated

with polysorbate 80, they were non-hemolytic up to the concentration tested here (3mg/mL), independently of their loading and functionalization.

Concerning opsonization, a first study of PLGA nanoparticle stability in different buffers (PBS and VBS[2+]), including human serum (HS) in the VBS[2+] buffer, confirmed a modification of physico-chemical characteristics (size and surface charge) of all types of nanoparticles when serum was included (Table 2) which could be an indication of serum protein interaction with nanoparticle surface, as previously reported [19]. The size decrease found for loperamide-loaded nanoparticles in the presence of serum had not been previously described. It could be attributed to some kind of interaction of loperamide molecules with HS constituents, as well as to a shrinkage of the polymeric matrix. Nanoparticle surface charge resulted in expected values taking into account the surface materials nature [32,40-41].

Studying specific proteins (fibrinogen and BSA), differential behaviors were found for each, as previously stated by *Vauthier et al.,* [12] who attributed the differential protein adsorption as due to the differences in their conformation (size, shape and charge; as assessed by protein data bank (PDB).

Fibrinogen, a rod-like shape anionic protein, only produces aggregation when nanoparticle surfaces were cationic (Table 3). The slight increase on the nanoparticle size found for non-aggregated dispersions may be due to fibrinogen adsorption. However, the size decrease found for loperamide-loaded nanoparticles was not expected (Table 3). An interaction of the fibrinogen with the drug could be hypothesized, producing shrinkage of

the polymeric nanoparticle corona. This size decrease represents a confirmation of the above-mentioned possible interaction of loperamide with components of the serum.

The adsorption of BSA onto nanoparticle surface has been widely reported for different kinds of polymeric nanoparticles [12,16,24,39], including PLGA nanoparticles [42]. In the present work, adsorptions typically lower than 10mg/mL of BSA (300 μg/cm^2) were found (Figure 1 and Table 6). Comparing different nanoparticle types, only 8D3-functionalized nanoparticles showed much lower saturation concentrations than other nanoparticle types (between 100 – 300 μg/cm^2). As expected, the BSA adsorption depended mainly on the nanoparticle surface. Nanoparticle sizes increased notably after the BSA incubation, except NP(LOP), which is in good agreement with fibrinogen size determinations. The nanoparticle size increase was an indication of the BSA adsorption onto the nanoparticle surface instead of within the polymeric matrix, as previously reported for other polymeric nanoparticles [16].

Comparing with previous bibliography, similar BSA concentrations of saturation were found in previous studies considering polymeric nanoparticles [12,43]. Studies concerning PLGA nanoparticles also exist [23-25,39]. Most of them [23,25,39] consist on comparative studies between non-coated and coated PLGA nanoparticles (e.g. PEGylation or thiolation). All they stated a lower protein adsorption after the nanoparticle functionalization due to the reduction of the hydrophobicity of nanoparticle surface. The protein interaction dependence on the nanoparticle surface hydrophobicity is in good agreement with previous reports [44-45].

BSA density per surface unit was studied in depth (Table 6). Around a hundred BSA molecules were adsorbed per unit of surface in most of nanoparticle dispersions. However, for loperamide-loaded nanoparticles, the BSA adsorption density increased up to values typically higher than a thousand (Table 6). For NP(LOP) and NP(8D3), two saturation values were set, corresponding to each of the saturation plateaux (Figure 1). Comparing experimental N_{BSA} with theoretical values obtained from the dimensions of the BSA molecule (Figure 3), experimental adsorption of NP(G2SN) and NP(C6,G2SN) are closer to the values of a BSA contact by the side with its small surface ($32nm^2$) (Table 6). In contrast, NP(LOP,G2SN) showed numbers of BSA adsorption closer to the BSA contact by the side with higher surface ($64nm^2$). In addition, for NP(LOP) and NP(8D3), at low BSA concentration, the BSA molecules interact with nanoparticles by their bigger surface, but when BSA concentration is increased, a high osmotic pressure might be caused by excess BSA molecules, resulting in a shift to a BSA interaction by their smaller surface (Figure 3, from a) to b)). In a first analysis of the results, a monolayer of BSA molecules around each nanoparticle was suggested. However, for NP(LOP), a multilayer BSA adsorption could be hypothesized since the number of BSA molecules adsorbed per surface unit was much higher than those calculated theoretically. The BSA adsorption in a multilayer conformation was previously envisaged [43] and attributed to an enhanced affinity of the nanoparticle components for the BSA molecules.

Table 6: Nanoparticle hydrodynamic size, $[BSA]_{saturation}$, and number of BSA molecules adsorbed onto an equivalent surface (N_{BSA}), for different types of nanoparticles at a

nanoparticle surface of 1000 cm^2. Initial sizes were used for any calculation. Parameters of

NP and NP(C6) could not be calculated, since a change in the ζ potential was not observed.

Nanoparticle set	Hydrodynamic radii (nm)		[BSA]$_{saturation}$		N$_{BSA}$ (BSA/μm^2) * 10^3		
					Theoretical		
	Initial	After BSA incubation	mg/mL	μg/cm^2	S$_{BSA}$ = 64nm^2	S$_{BSA}$ = 32nm^2	Experimental
NP (G2SN)	26	125	3	150	79	157	179
NP (C6,G2SN)	24	75	2	100	79	157	118
NP (LOP)	100	45	5	250	1963	3925	2196
			20	1000			8784
NP (LOP,G2SN)	98	115	2	100	1963	3925	878
NP (8D3)	21	150	0.75	37.5	79	157	44
			10	500			592
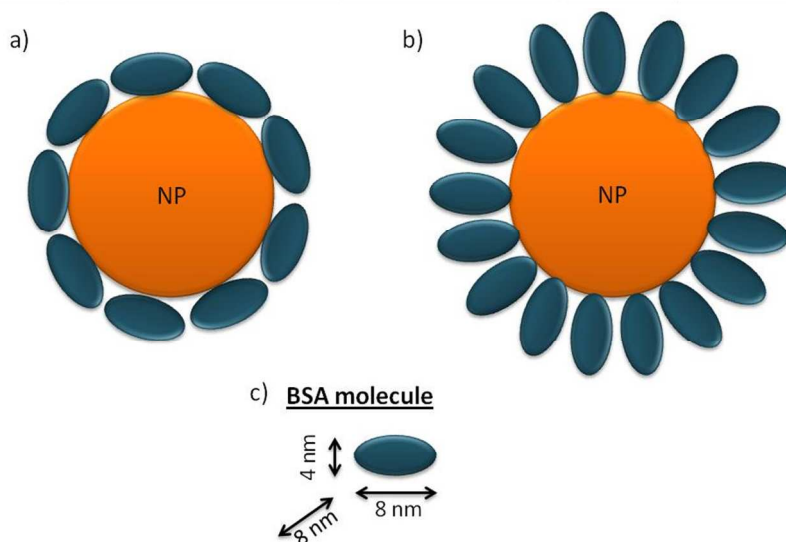
Figure 3: Schematic representation of the two possible orientations of BSA molecules onto

nanoparticle surface. a) Surface in contact = 64 nm2; b) Surface in contact = 32 nm2; and

c) Dimensions of the BSA molecule.

The nanoparticle influence on the coagulation is another important factor to take into account before the intravenous administration [2,11]. Although NP(G2SN) produced a marked anticoagulant effect at the highest concentration (3mg/mL), all nanoparticles studied can be administered with safety conditions concerning coagulation issues at concentrations up to 1mg/mL and most of them even at concentrations up to 3mg/mL; which is a markedly higher concentration than those reported previously [10-11,20]. Therefore, our nanoparticles could be more appropriate than previously designed nanoparticles for the intravenous administration in terms of coagulation.

Since fibrinogen is a critical component of the coagulation cascade, results concerning fibrinogen aggregation and those for the coagulation cascade should agree [6,19]. Only NP(G2SN) produced fibrinogen aggregation and an anticoagulant effect simultaneously at higher concentration . Since fibrinogen forms aggregates with the nanoparticles, it may be not accessible to be used by the coagulation cascade, resulting in an anticoagulation effect.

The activation of the complement cascade is another important factor to study before the intravenous administration, since it gives an indication of the nanoparticle recognition by the immune system [6,17]. As described in the results section, the complement activation depended on the nanoparticle loading but in a higher degree on their functionalization (Table 4). Different functionalizations tested showed different level of complement activation. It is worth remarking that the complement cascade includes an amplifying system, therefore, it may be induced by small changes of conditions, as shown in this

study. Enhancement of complement activation by antibody functionalization was consistent with results reported in previous literature [17,46-47]. *Pham et al.,* [47] stated that the classical pathway of the complement system, where C3 protein is also involved, is usually activated due to the presence of antibodies. In addition, *Moghimi et al.,* [17], found an increase in the complement activation when nanoparticles were antibody-functionalized. Regarding NP nanoparticles, previous studies reported similar and higher values of complement activation for polymeric nanoparticles [11-12,34-35,38,48]. *Bertholon et al.,* [38], for example, found activation percentages up to 40%, for certain types of dextran-coated nanoparticles. Previous studies of PLGA nanoparticles complement activation [11,26,28,39] reported a weak to high activation of the complement system, attributed to the PLGA hydrophobicity. Our nanoparticles, independently of the loading / functionalization, produced lower activations of the complement system. Although it is believed that nanoparticles with sizes below 100 nm are less uptaken by macrophages and less recognized by opsonins [34-35], our results were consistent with those of *Bertholon et al.,* [38], who found no relation between the nanoparticle size and the activation of the complement system.

Aiming to reach a target tissue located outside organs of the immune system, it is desired that the nanoparticles will not be detected by the immune system [14,38]. The *in vitro* activation of the complement system was previously reported to directly depend on the concentration of the nanoparticles [49-50]. Therefore, NP(8D3) nanoparticles could be used at lower concentrations, thus, their activation of the complement system would be reduced. In addition, as compared with previous studies [11-12,26,39], our NP

nanoparticles represent more appropriate systems for the intravenous administration in terms of activation of the immune system, since they would not activate the complement system [18].

Previous studies stated a relationship between the complement activation and the protein adsorption, since the complement system is involved in opsonization (clearance of protein-coated nanoparticles) [11-12,14,38-39]. Nevertheless, factors affecting both parameters have been not fully described. Some authors state that the smaller the nanoparticles, the lower the opsonization [9], as indicated above. This was only found in the present work for studies of the BSA adsorption, where the number of molecules of BSA adsorbed per surface unit was larger for bigger nanoparticles (Table 6). Other authors reported dependence between the nanoparticle surface charge and protein adsorption / opsonization [10,51]. In the present work, only the fibrinogen aggregation depended on the nanoparticle surface charge. A more general dependence between the surface functionalization and the opsonization has been reported by other authors [10,39]. In the present work, BSA and fibrinogen adsorption, as well as the complement activation were dependent on the nanoparticle surface.

4. Experimental

4.1. **Materials**

Poly-(lactid-co-glycolic) acid (PLGA) with a lactic to glycolic ratio of 75/25 and a molecular weight of 10,000 Da was purchased from Evonik (Resomer 752H). Polysorbate 80 was a kind gift from Croda (Tween 80 ®). Bovine serum albumin (BSA), agarose, the salts of the

buffers (Sodium chloride, disodium monophosphate dehydrate and sodium diphosphate dehydrate for phosphate buffered saline (PBS: 10mM, NaCl 140mM, KCl 25mM, pH=7.5), for the tricine buffer (1mM calcium lactate, 63mM TRIS and 27mM tricine) and for the veronal buffer VBS^{2+} (0.15mM calcium chloride, 0.5mM magnesium chloride), human fibrinogen, the complement C3 antiserum rose in goat, Comassie Blue and acetic acid were purchased from Sigma. human serum (HS) was obtained from Etablissement Française du Sang, Kremblin Bicêtre, France. Ethyl acetate was purchased from Merck. HemosIL SynthASil and HemosIL RecombiPlasTin 2G from Instrumentation Laboratory Company, Bedford MA, USA. Water was MillQ filtered.

4.2. Methods

4.2.1. Nanoparticle preparation

PLGA nanoparticles were prepared from nano-emulsion templating, using the phase inversion composition (PIC) emulsification method to prepare polymeric nano-emulsions [29] followed by solvent evaporation to obtain nanoparticles as described in previous bibliography of our group [30-31]. A purification step was added afterwards to remove the traces of surfactant excess. All nanoparticles were dispersed in an isotonic phosphate buffered saline (PBS) solution, at the physiological pH (7.4) and osmolality (300mOsm/kg). The nano-emulsion system used consisted of PBS (W)/ polysorbate 80 (S)/ [4wt% PLGA in ethyl acetate] (O). Different types of PLGA nanoparticles were prepared, described in Table 1. Differences between the types are their loadings and functionalizations. Two different compounds were included as loading: the fluorescent dye Coumarin 6 (C6), with

the future aim to use the nanoparticles as imaging agents; and the drug loperamide

hydrochloride (LOP), with the aim to use nanoparticles as drug carriers. As

functionalization agents, carbosilane cationic dendrons of the second generation (G2SN)

and the anti-transferrin receptor monoclonal antibody (8D3) were used, with the aim to

passively and actively vectorize nanoparticles to the blood-brain barrier, respectively. The

loadings were added as a component of the oil phase of the template nano-emulsions,

thus achieving high entrapment efficiencies. The functionalization agents were covalently

attached to PLGA after nanoparticle formation, by means of the carbodiimide reaction

[31].

Table 1: Identification codes for all types of nanoparticles used in this work.

Identification	Loading	Functionalization
NP	None	None
NP(G2SN)	None	G2SN dendron
NP(8D3)	None	8D3 antibody
NP(C6)	Coumarin 6	None
NP(C6,G2SN)	Coumarin 6	G2SN dendron
NP(LOP)	Loperamide	None
NP(LOP,G2SN)	Loperamide	G2SN dendron

4.2.2.   **Characterization of nanoparticles size and surface charge**

29

Nanoparticle hydrodynamic sizes were measured using the dynamic light scattering technique (DLS) while surface charge was assessed by means of the ζ potential. The surface charge was obtained using the Hückel-Onsager equation, from the electrophoretic mobility determinations [37]. Both measurements were carried out using the ZetaSizer Nano (Malvern, France). Nanoparticles were diluted 1/20 with water to accomplish the conductivity requirements of the equipment. Values are given as means and standard deviations.

4.2.3. Stability of nanoparticle dispersions in buffers

The stability of nanoparticle dispersions was measured by means of size and ζ potential determination, at the initial preparation time and after 1 hours of incubation at 37ºC in different buffer. The PBS, VBS^{2+} and VBS^{2+} + HS were used, since these were the buffers used for further experimentation.

4.2.4. Interaction of nanoparticles with fibrinogen

Nanoparticle dispersions were incubated for 1h with fibrinogen solutions at 0 and 2 mg/mL fibrinogen concentration (Human fibrinogen from Sigma) dissolved in PBS 100mM, pH 7.4, at a nanoparticle / fibrinogen solution volume ratio of 1/10. The macroscopic behavior of the dispersion during fibrinogen addition was observed to follow occurrence of precipitation. The microscopic aspect of the dispersions containing 2mg/mL of fibrinogen was observed with an optical microscope using the phase contrast mode (Olympus BH2). Dispersions that appeared homogenous by microscopic observations were characterized by means of DLS and ζ potential, using a Malvern Z Sizer Nano Z [37].

4.2.5. **Interaction of nanoparticles with bovine serum albumin (BSA)**

Nanoparticles at a concentration of 1000 cm^2/mL were incubated with different concentrations in a range from 0 to 40 mg/mL of BSA in PBS, for 10 minutes, at 37ºC, in a total volume of 50 μL. After incubation, the BSA adsorption was determined by means of ζ potential measurements. Adsorption isotherms were plotted to study the BSA concentration of saturation. The adsorption concentrations were also evaluated as mass per cm^2 of nanoparticle surface, with the aim to compare the adsorption between the different nanoparticles and with theoretical calculations. In addition, the size of the nanoparticles was evaluated before and after the incubation with BSA at the saturation concentration. Theoretical calculations were performed to calculate the number of BSA molecules adsorbed per surface unit for different nanoparticle types (N_{BSA}). N_{BSA} was calculated from the experimental values obtained, taking into account the BSA saturation concentration and nanoparticle dimensions. It was also calculated the theoretical N_{BSA} taking into account the dimensions of the BSA molecule [12,16]. Since BSA has around 8x8x4 nm, two surfaces could be in contact with nanoparticle surface (32 or 64nm^2). Therefore, two theoretical calculations were possible.

4.2.6. **Interaction of nanoparticles with the coagulation cascade**

Influence of the addition of nanoparticles in plasma on the coagulation cascade was assessed *in vitro* by measuring the activated partial thromboplastin time (APTT), which is a measure of the intrinsic coagulation pathway, and the prothrombin time (PT), which is a measure of the extrinsic coagulation pathway. Basal values of the APTT range between 25

– 35 seconds while PT range between 12 – 15 seconds [19,21]. The experimental protocol used was described by *Dobrovolskaia et al.*, [19], although slight modifications were introduced in the present work. In brief, blood from healthy donors was collected in Vacutainer tubes (BD Diagnostics Franklin Lakes, New Jersey) containing sodium citrate as anticoagulant. The plasma was isolated by recollecting the supernatant of the centrifuged blood at 3,000 rpm, 10 min at 25ºC. Then, plasma was subjected to clotting tests, both measured using a Coagulometer KC1. 10 µL of each sample were added to 100µL of plasma and incubated for 30 minutes, under continuous shaking, at 37ºC. Each sample was tested in triplicate. For the PT assessment, once a sample was placed into the coagulometer, 200 µL of the phospholipid calcium thromboplastin were added and the coagulation time was automatically assessed. For the APTT assessment, 100 µL of cephalin, a negatively charged phospholipid acting as contact activator, were added to the sample previously placed in the coagulometer. The mixture was incubated for 2 minutes, followed by the addition of 100 µL of calcium chloride to activate the clot formation; and measurement of the coagulation time.

4.2.7. **Interaction of nanoparticles with the complement cascade**

Activation of the complement system induced by the different types of nanoparticles was evaluated using a 2D immunoelectrophoresis method, as described in the previous literature [12,38].

In brief, 50µL of the nanoparticle dispersion at a nanoparticle concentration of 1000 cm^2 per mL, in PBS (calculated by their hydrodynamic sizes) were incubated with 50µL of

human serum and 50μL of veronal buffer containing 0.15mM calcium chloride and 0.5mM magnesium chloride, for 1 h, at 37ºC. After incubation, 5μL of each sample were placed to a first electrophoresis on 1% agarose gels. The second dimension electrophoresis was carried out on Gelbond® films in 1% agarose gel plates containing a polyclonal antibody to human C3 (Complement C3 antiserum rose in goat, Sigma, France), recognizing both C3 and C3b. the films were dried and stained as reported for BSA studies, to reveal the presence of C3 and C3b which have reacted with the antibody (Sigma). The complement activation percentage was calculated from the ratio between the area of the peak attributed to C3b over the sum of the areas of the peaks attributed to C3 and C3b. 100% indicated the total activation and 0% the spontaneous activation measured in absence of nanoparticles (normalized values with the positive and negative controls).

4.2.8. **Determination of the hemolysis**

Erythrocytes or human red blood cells (RBS), kindly provided by healthy volunteers that gave their informed consent (Blood Bank, Hospital Clinic i Provincial de Barcelona, Spain), were obtained by centrifugation (10 min, 867 g). All experiments were performed in compliance with the Ethical Committee of the University of Barcelona, which approved them before the starting of the experimental procedures, following the Guidelines of the European Community Council in accordance with the Nuremberg Code (Directive 2004/23/EC). Supernatants were ruled out and the erythrocytes were resuspended in PBS to remove other cells and traces of plasma. This washing step was repeated trice and then, erythrocytes were dispersed in PBS, at a concentration of 8 x 10^9 cells/mL. The

hemolytic activity was assessed by spectroscopic experiments [22]. 1 mL of each sample (3mg/mL of nanoparticles) was placed in an eppendorf, and mixed with 25 μL of RBC. The mixture was incubated at 25ºC, under continuous agitation for the required time (10 minutes or 24 hours) and then centrifuged for 5 minutes, at 867 g at room temperature. The percentage of hemolysis was spectroscopically assessed by comparing the absorbance (λ=540 nm) of the samples with the positive (distilled water) and negative (PBS) controls. The results are expressed as the percentage of hemolysis caused.

4.2.9. **Microscopic observations**

Optical microscopy was used to observe the presence of aggregates in samples in which fibrinogen was added. Observations were performed using the phase contrast mode (Olympus BH2) to highlight occurrence of microscopic phase separation in samples.

5. **Conclusion**

In conclusion, the interaction with two model blood proteins (BSA and fibrinogen), the activation of the coagulation and complement cascades and the production of hemolysis have been studied for diverse types of PLGA nanoparticles as a function of their loading and functionalization. Nanoparticles tested in this work did not produce hemolysis, indicating that they do not induce toxicity to erythrocytes. The more appropriate nanoparticles to be intravenously administered were those without any loading and functionalization. The introduction of a loading produced a slight increase in the complement activation, while the nanoparticle functionalization produced an increase of this activation. Loperamide enhancement of BSA adsorption onto nanoparticle surface

was attributed to the bigger sizes of loperamide-loaded nanoparticles. The G2SN

nanoparticle functionalization affected the fibrinogen aggregation as well as the

coagulation cascade, due to the positive charges of the surface. Therefore, some

modifications should be included onto nanoparticle surface of G2SN-functionalized

nanoparticles for their use as intravenous delivery systems, while other nanoparticles (e.g.

loperamide-loaded nanoparticles) are already appropriate for the intravenous

administration.

6. Acknowledgements

7. References

1. C Pinto Reis, RJ Neufeld, AJ Ribeiro, F Veiga. Nanoencapsulation I. Methods for
    preparation of drug-loaded polymeric nanoparticles. Nanomed: Nanotechnol, Biol and
    Med 2006;**2(1**):8–21.

2. MA Dobrovolskaia, P Aggarwal, JB Hall, SE McNeil. Preclinical Studies To Understand Nanoparticle Interaction with the Immune System and Its Potential Effects on Nanoparticle Biodistribution. Mol Pharm 2008;**5(4)**:487 – 495.

3. A Kumari, SK Yadav, SC Yadav. Biodegradable polymeric nanoparticles based drug delivery systems. Colloids Surf B 2010; **75(1)**:1–18.

4. S Mura, P Couvreur. Nanotheranostics for personalized medicine. Adv Drug Deliv Rev 2012;**64(13)**:1394–1416.

5. J Nicolas, S Mura, D Brambilla, N Mackiewicz, P Couvreur. Design, functionalization strategies and biomedical applications of targeted biodegradable/biocompatible polymer-based nanocarriers for drug delivery, Chem Soc Rev 2013;**42**:1147 – 1235.

6. MA Dobrovolskaia, S McNeil. (2013). Handbook of immunological properties of engineered nanomaterials, Frontiers in Nanobiomedical esearch, SAIC-Frederick, Inc., USA.

7. J Kreuter. Nanoparticle-based drug delivery systems. J Control Release 1991;**16**:169 – 176.

8. D Labarre, C Vauthier, C Chauvierre, B Petri, R Müller, MM Chehimi. Interactions of blood proteins with poly(isobutylcyanoacrylate) nanoparticles decorated with a polysaccharidic brush. Biomaterials 2005;**26**:5075–5084.

9. R Alyautdin, I Khalin, MI Nafeeza, MH Haron, D Kuznetsov. Nanoscale drug delivery systems and the blood-brain barrier, Int J Nanomed 2014;**9**:795 – 811.

10. M Dobrovolskaia, S McNeil. Immunological properties of engineered nanomaterials, Nature Nanotech 2007;**2**:469 – 478.

11. E Cenni, D Granchi, S Avnet, C Fotia, M Salerno, D Micieli, MG Sarpietro, R Pignatello, F Castelli, N Baldini. Biocompatibility of poly(D,L-lactide-co-glycolide) nanoparticles conjugated with alendronate. Biomaterials 2008;**29**:1400e1411.

12. C Vauthier, B Persson, P Linder, B Cabane. Protein adsorption and complement activation for di-block copolymer nanoparticles. Biomaterials 2011;**32**:1646 – 1656.

13. T Blunk, DF Hochstrasser, JC Sanchez, BW Miiller, RH Miillelj. Colloidal carriers for intravenous drug targeting: Plasma protein adsorption patterns on surface-modified latex particles evaluated by two-dimensional polyacrylamide gel electrophoresis. Electrophoresis 1993;**14**:1382-1387.

14. M Cavadas, A González-Fernández, R Franco. Pathogen-mimetic stealth nanocarriers for drug delivery: a future possibility, Nanomed: Nanotech, Biol Med 2011;**7(6):**730–743

15. I Lynch, KA Dawson. Protein – nanoparticle interactions, NanoToday 2008;**3(1-2)**: 40 – 47.

16. C Vauthier, P Lindner, B Cabane. Configuration of bovine serum albumin adsorbed on polymer particles with grafted dextran corona. Colloids Surf B 2009;**69**:207–215.

17. SM Moghimi, AJ Andersen, D Ahmadvand, PP Wibroe, TL Andresen, AC Hunter. Material properties in complement activation, Adv Drug Del Rev 2011;**63**:1000 – 1007.

18. J Sbezini, P Bedocs, D Csukás, L Rosivall, R Bünger, R Urbaniks. A porcine model of complement-mediated infusion reactions to drug carrier nanosystems and other medicines. Adv Drug Del Rev 2012;**64**:1706 – 1716.

19. MA Dobrovolskaia, AK Patri, J Zheng, JD Clogston, N Ayub, P Aggarwal, BW Neum, Hall JB, McNeil S. Interaction of colloidal gold nanoparticles with human blood: effects on particle size and analysis of plasma protein binding profiles. Nanomedicine 2009;**5**: 106 – 117.

20. H Sahli, Tapon-Bretaudière, AM Fischer, C Sternberg, G Spenlehauer, T Verrecchia, D Labarre. Interactions of poly(lactic acid) and poly(lactic acid-co-ethylene oxide) nanoparticles with the plasma factors of the coagulation system. Biomaterials 1997; **18**:281 – 288.

21. C Salvador-Morales, L Zhang, R Langer, OC Farokhzad. Immunocompatibility properties of lipid–polymer hybrid nanoparticles with heterogeneous surface functional groups. Biomaterials 2009;**30**:2231 – 2240.

22. RM Aparicio, MJ García-Celma, MP Vinardell, M Mitjans. In vitro studies of the hemolytic activity of microemulsions in human erythrocytes. J Pharm Biomed Anal 2005;**39**:1063–1067.

23. RH Müller, KH Wallis. Surface modification of i.v. injectable biodegradable nanoparticles with poloxamer polymers and poloxamine 908. Int J Pharm 1993**;89**: 25-31

24. S Stolnik, SE Dunn, MC Garnett, MC Davies, AGA Coombes, DC Taylor, MP Irving, SC Prkiss, TF Tadros, SS Davis, L Illum. Surface modification of poly(lactide-co-glycolide) nanospheres by biodegradable poly(lactide)-poly(ethylene glicol) copolymers. Pharm Res 1994; **11(12):** 1800 – 1808.

25. R Gref, A Domb, P Quellec, T Blunk, RH Müller, JM Verbavatz, R Langer. The controlled intravenous delivery of drugs using PEG-coated sterically stabilized nanospheres. Adv Drug Del Rev 2012;**64**:316 – 326.

26. VCF Mosqueira, P Legrand, A Gulik, O Bourdon, R Gref, D Labarre, G Barratt. Relationship between complement activation, cellullar uptake and surface physicochemical aspects of novel PEG-modified nanocapsules. Biomaterials 2001;**22**:2967 – 2979.

27. D Kim, H El-Shall, D Dennis, T Morey. Interaction of PLGA nanoparticles with human blood constituents. Colloids Surf B 2005;**40**:83 – 91.

28. SM D'Addio, W Saad, SM Ansell, JJ Squiers, DH Adamson, M Herrera-Alonso, AR Wohl, TR Hoye, CW Macosko, LD Mayer, C Vauthier, RK Prud'homme. Effects of block copolymer properties on nanocarrier protection from in vivo clearance. J Control Release 2012;**162(1):**208–217.

29. C Solans, I Solè. Nano-emulsions: Formation by low-energy methods, Curr Opin Colloid Interface Sci 2012;**17**:246 – 254.

30. G Calderó, MJ García-Celma, C Solans. Formation of polymeric nano-emulsions by a low-energy method and their use for nanoparticle preparation. J Colloid Interface Sci 2011;**353(2):**406–411.

31. C Fornaguera, S Grijalvo, M Galán, E Fuentes-Paniagua, FJ de la Mata, R Gómez, R Eritja, G Calderó, C Solans. Novel non-viral gene delivery systems composed of carbosilane dendron functionalized nanoparticles prepared from nano-emulsions as non-viral carriers for antisense oligonucleotides. Int J Pharm 2015;**478(1):**113 - 123 .

32. S Stolnik, MC Garnett, L Illum, M Bousta, M Vert, SS Davis. The colloidal properties of surfactant-free biodegradable nanospheres from poly(b-malic acid-co-benzyl malate)s and poly(lactic acid-co-glycolide). Colloids Surf A 1995;**97:**235 – 245.

33. C Vauthier, K Bouchemal. Methods for the preparation and manufacture of polymeric nanoparticles, Pharm Res 2009;**26(5):**1025 – 1058.

34. SA Kulkarni, SS Feng. Effects of particle size and surface modification on cellular uptake and biodistribution of polymeric nanoparticles for drug delivery, Pharm Res 2013;**30:**2512 – 2522.

35. B Neha, B Ganesh, K Preeti. Drug delivery to the brain using polymeric nanoparticles: a review, Int J Pharm Life Sci 2013;**2(3):**107 – 132.

36. J Kreuter. Drug delivery to the central nervous system by polymeric nanoparticles: What do we know?, Adv Drug Deliv Rev 2014;**71**:2 – 14.

37. AV Delgado, F González-Caballero, RJ Hunter, LK Koopal. Measurement and interpretation of electrokinetic phenomena, J Colloids Interface Sci 2007;**309**:194 – 224.

39

38. I Bertholon, C Vauthier, D Labarre. Complement activation by core-shell poly(isobutylcyanoacrylate)-polysaccharide nanoparticles: influences of surface morphology, length and type of polysaccharide, Pharm Res 2006;**23(6):**1313 – 1323.

39. YM Thasneem, S Sajeesh, CP Sharma. Effect of thiol functionalization on the hemo-compatibility of PLGA nanoparticles, J Mat Res 2011;**99(4):**607 – 617.

40. O Harush-Frenkel, N Debotton, S Benita, Y Altschuler. Targeting of nanoparticles to the clathrin-mediated encodytic pathway, Biochem Biophys Res Comm 2007;**353**:26 – 32.

41. RP Singh, P Ramarao. Accumulated polymer degradation productes as effector molecules in cytotoxicity of polymeric nanoparticles, Toxicol Sc 2013;**136(1):**131 – 143.

42. T Verrecchia, G Spenlehauer, DV Bazile, A Murry-Brelier, Y Archimbaud, M Veillard. Non-stealth (poly(lactic acid/albumin)) and stealth (poly(lactic acid-polyethylene glycol)) nanoparticles as injectable drug carriers, J Control Release 1995;**36**:49 – 61.

43. JC Olivier, C Vauthier, M Taverna, D Ferrier, P Couvreur. Preparation and characterization of biodegradable poly(isobutylcyano acrylate) nanoparticles with the surface modified by the adsorption of proteins, Colloids Surf B 1995;**4:**349 – 356.

44. DF Moyano, K Saha, G Prakash, B Yan, H Kong, M Yazdani, VM Rotello. Fabrication of Corona-Free Nanoparticles with Tunable Hydrophobicity, ACS Nano 2014;**8(7):** 6748–6755.

45. K Chen, S Rana, DF Moyano, Y Xu, X Guo, VM Rotello. Optimizing the selective recognition of protein isoforms through tuning of nanoparticle hydrophobicity, Nanoscale 2014;**6:**6492-6495.

46. JD Byrne, T Betancourt, L Brannon-Peppas. Active targeting schemes for nanoparticle systems in cancer therapeutics, Adv Drug Del Rev 2008;**60(15):**1615 – 1626.

47. CTN Pham, LM Mitchell, JL Huang, CM Lubniewski, OS Schall, JK Killgore, D Pan, SA Wickline, GM Lanza, DE Hourcade. Variable Antibody-dependent Activation of Complement by Functionalized Phospholipid Nanoparticle Surfaces, J Biol Chem 2011;**286:**123 – 130.

48. C Zandanel, C Vauthier. Poly(isobutylcyanoacrylate) Nanoparticles Decorated with Chitosan: Effect of Conformation of Chitosan Chains at the Surface on Complement Activation Properties, J Colloid Sci Biotech 2012;**1(1):** 68-81(14).

49. SM Moghimi, J Szebeni. Stealth liposomes and long circulating nanoparticles: critical issues in pharmacokinetics, opsonization and protein-binding properties, Progress Lipid Res 2012;**42**:463 – 478.

50. A Vonarbourg, C Passirani, P Saulnier, JP Benoit. Parameters influencing the stealthiness of colloidal drug delivery systems, Biomaterials 2008;**27**:4356 – 4373.

51. R Minchin. Nanomedicine: Sizing up targets with nanoparticles, Nature Nanotech 2008;**3:** 12 – 13.